Journal of Materials Chemistry A

Accepted Manuscript

ROYAL SOCIETY OF CHEMISTRY

www.rsc.org/materialsA

Journal Name

RSCPublishing

ARTICLE

Fe@C core-shell and Fe@C yolk-shell particles for effective removal of 4-chlorophenol

Cite this: DOI: 10.1039/xoxxoooooox

Xiang Li,[a] Fangyuan Gai,[b] Buyuan Guan,[a] Ye Zhang,[a] Yunling Liu[a] and Qisheng Huo[a]*

Received ooth January 2012,
Accepted ooth January 2012

DOI: 10.1039/xoxxoooooox

www.rsc.org/

Fe@C core-shell particles were successfully synthesized by coating Fe_2O_3 particles with resorcinol–formaldehyde resins (RFs) and then calcining to make the RFs carbonize, and at the same time reduce the core to Fe. Furthermore, we design and synthesize Fe@C yolk-shell particles to increase the number of active sites on the Fe surface. Compared with pure Fe material, the Fe in these particles possesses high surface area without serious aggregation. Then the 4-chlorophenol removal tests suggest both these kinds of particles can degrade chlorophenol rapidly and thoroughly based on the Fenton-like reaction. Especially for Fe@C yolk-shell particles, the chlorophenol can be degraded to the concentration below HPLC detection limit (< 0.5 mg/l) within 12 minutes. The magnetic property and good stability endow it with promising potential in water treatment.

Introduction

Over the past several decades, contamination of water has brought an increasing number of environment and health risks, and drew more and more attention from both the public and the researchers.[1-3] Among those contaminants, chlorophenols constitute a particular group of priority toxic pollutants listed by the U.S.EPA in the Clean Water Act for being toxic and hardly biodegradable.[4-7] Chlorophenols have been used commonly as preservative agents for wood and also been employed in a great deal of industrial production, such as manufacturing of pesticides and so on.[8-10] However, chlorophenol, as a kind of soluble small organic molecular which is difficult to remove by sedimentation, has raised extensive concern to degrade it.

Until now, methods for chlorophenol degradation involve reagents oxidation (such as manganese oxides, ozone),[4, 11] electro-catalytic oxidation method,[12, 13] photo-catalytic degradation method,[14-16] absorption by porous materials such as functionalized multiwall carbon nanotubes,[17-19] biochemical method with oxidative enzymes such as laccase and so on.[20-22] Among these techniques, Fenton regent (a mixture of ferrous ion and hydrogen peroxide) is an absolutely efficient method because it can degrade most organic contaminants to less toxic and more biodegradable species without the need of additional assistants such as UV or ultrasound.[5, 23-26] Furthermore, zero valent iron (ZVI) material, as a kind of heterogeneous catalyst, is used to induce so-called Fenton-like reaction.[27, 28] It not only can perform as well as ferrous homogeneous catalyst, but also can be controlled easily and retained.[29, 30] What is more, ZVI is both low-cost and storable, which make it more practical in the treatment of polluted water.[31-33]

Recently, many researches have focused on improving the performance of treatment of polluted water by ZVI.[8, 28, 34-38] Wang et al. synthesized nanoscale Fe which reveals much better stability and durability for degrading chlorophenol compared with common iron particles.[34] Chen et al. doped Fe with Pd and found that the dechlorination rate increased with increased Pd loading.[35] Dai et al. used ultrasound in combination with iron to degrade organic contaminants and testified its high performance in the removal of the pollutant.[36] Li et al. remarkably enhanced the reactivity of removing chlorophenol by immobilizing nano ZVI on organobentonite, which is due to a synergetic effect.[37] Zhang et al. synthesized a novel material, $Fe@Fe_2O_3$ nanowires, and investigated its reactivity on degrading chlorophenol.[38] Besides, Kiwi et al.[8] and Cao et al.[28] immobilized Fe on the Nafion membrane and in the ordered mesoporous carbon respectively, which can also improve the performance of degrading chlorophenol. However, taking advantage of core-shell or yolk-shell structure to promisingly increase the number of the active sites on the iron surface and therefore contributing to a rapid degradation of chlorophenol has been relatively less reported.

[a]*State Key Laboratory of Inorganic Synthesis and Preparative Chemistry, College of Chemistry, Jilin University, Changchun 130012, China. E-mail: huoqisheng@jlu.edu.cn; Tel: +86-431-85168602*

[b]*Department of petroleum and chemical engineering, Dalian University of Technology, 2 Dagong Road, New District of Liaodong Bay, Panjin 124221, China*

Core-shell particles have wide applications since they are multiply functional.[39, 40] Carbon material is used for the shell of metal@carbon particles.[41-44] Previously, some great methods to form carbon shell have been reported.[45-47] For example, Dai et al. have developed a facile method for preparing hollow carbon sphere with dopamine.[45] Lu et al. have demonstrated a confined nanospace pyrolysis method to produce dispersible and uniform hollow carbon spheres.[46] Fuertes et al. have presented a one-step method to envelop SiO_2 with resorcinol–formaldehyde resins (RFs).[47] Among so many studies, phenol–formaldehyde resin is a considerable choice for its good carbon yield and easy handling.

Herein, we present our synthesis of Fe@C core-shell particle and Fe@C yolk-shell particle by utilizing the RFs to form a shell around the core and then calcining the RFs into carbon. It is the carbon shell that as a reducing agent to transform Fe_2O_3 into Fe, and simultaneously, the carbon shell avoids a serious aggregation of Fe caused by its own magnetic property. In the chlorophenol removal test, these particles show considerably excellent performance. Especially Fe@C yolk-shell particles can provide both rapid degradation of 4-chlorophenol within 12 minutes and a total removal to a level below the detection limit of HPLC. This reveals that yolk-shell structure endows these particles with abundant active sites and thus high reactivity. Besides, these particles are stable and renewable, which can be preserved in the air for at least three months and be regenerated for several cycles.

Experimental

Materials

Resorcinol (99.5%) and formalin solution (37~40 wt.%) were purchased from Xilong Chemical Co. LTD. Cetyltrimethylammonium bromide ($C_{16}TMA^+Br^-$, 99.0 %) was obtained from Huishi Biochemical Reagent Company of China. 4-chlorophenol (4-CP 99.5%) was purchased from Aladdin Industrial Inc. $FeCl_3$ (97.0%) and Tetraethyl orthosilicate (TEOS, 99%) were purchased from Sinopharm Chemical Reagent Co., Ltd. C_2H_5OH (99.7%), ammonia (25~28 wt.%) and hydrogen peroxide (30%) were purchased from Beijing Chemical Works. NaH_2PO_4 (99.0%), isopropanol (99.7%) were obtained from Guangfu Chemical Co. LTD. All chemicals were used as received without any further purification.

Synthesis of rice-shaped Fe_2O_3 particles

The Fe_2O_3 core was synthesized following the method previously reported.[48, 49] Typically, 0.65g of $FeCl_3$ was dissolved in 200 ml of 10^{-4} M NaH_2PO_4 solution. Then the mixture was heated in an oven at 100 ^oC for 2 days. The rice-shaped Fe_2O_3 particles were collected by centrifuging and washed with deionized water and ethanol several times. Finally, the powder was dried in the air.

Synthesis of Fe_2O_3@RF and Fe@C core-shell particles

Fe_2O_3@RF core-shell particles were synthesized by previously reported method.[50-52] In brief the synthesis route is described as follows: 0.2 g of as-synthesized rice-like Fe_2O_3 particles was dispersed homogeneously in 17.6 ml of deionized water through ultrasonication for 15 min, followed by the addition of 0.57 g of $CTMA^+Br^-$, 0.087 g of resorcinol, 7.05 ml of ethanol and 25 µl of ammonia solution (25~28 wt.%). The mixture was stirred at 35 ^oC for 30 min to form a uniform suspension. Then, 125 µl of formalin solution was added to the mixture drop wise under stirring. After 6h of stirring at 35 ^oC, the mixture was cooled to the room temperature and aged overnight without stirring. After centrifugation and wash with deionized water and ethanol, the product Fe_2O_3@RFs was obtained. Then the powder was heated at 5 ^oC/min from room temperature to 150 ^oC and kept at this temperature for 1 h under nitrogen atmosphere. Next the temperature was raised to 600 ^oC at 5 ^oC/min and kept at this temperature for 2 h. Finally, the temperature was raised to 900 ^oC at 1 ^oC/min and kept for 1 h. Then it was cooled to the room temperature and Fe@C core-shell particles were obtained.

Synthesis of Fe_2O_3@SiO_2 particles

To coat the rice-shaped Fe_2O_3 particles with SiO_2, we employed a previously reported method.[48] Typically, 50 mg of as-synthesized rice-shaped Fe_2O_3 was dispersed in a mixture of isopropanol (100 ml), H_2O (20 ml) and ammonia solution (3 ml). Then 0.1 ml of TEOS was added under stirring. After 4 h, the product was collected by centrifugation and washed with deionized water and ethanol several times. Finally, the powder was dried in the air.

Synthesis of Fe_2O_3@SiO_2@RF and Fe_2O_3@SiO_2@C particles

Fe_2O_3@SiO_2@RFs were synthesized under similar reaction conditions of Fe_2O_3@RFs except replacing Fe_2O_3 with Fe_2O_3@SiO_2. Next, to obtain Fe_2O_3@SiO_2@Cs, the powder was heated at 5 ^oC/min from room temperature to 150 ^oC and was maintained this temperature for 1 h under nitrogen atmosphere. The temperature was then raised to 600 ^oC at 5 ^oC /min and maintained for 2 h.

Removal of SiO_2 and synthesis of Fe@C york-shell particles

To remove the SiO_2 in Fe_2O_3@SiO_2@Cs, the as-synthesized powder was added into the mixture of deionized water (20 ml) and ammonia (6 ml). Then the suspension was transferred into a Teflon-lined stainless steel autoclave. The autoclave was maintained at 85 ^oC for 5 h and then cooled to room temperature. The Fe_2O_3@Cs yolk-shell particles were collected by centrifuging and washed with deionized water and ethanol several times. After removing the SiO_2, the powder was heated at 5 ^oC/min from room temperature to 600 ^oC and then heated at 1 ^oC /min to 900 ^oC and maintained at this temperature for 1 h under nitrogen atmosphere. Then it was cooled to the room temperature and Fe@C yolk-shell particles were obtained.

Material characterization

The morphology of the particles was tested by scanning electron microscopy (JEOL JSM-6700F, 5 kV) and transmission electron microscopy (FEI Tecnai G2 s-twin D573, 200 kV). Powder X-ray diffraction (XRD) patterns were tested by Rigaku 2550 diffractometer with Cu-Kα radiation (λ=1.5418Å). The concentration of 4-CP was detected by high performance liquid chromatography (Agilent 1200). The CHN elemental analysis was tested by Elementar vario EL CUBE. Inductively coupled plasma mission spectroscopy was tested by ICP-OES, Perkin Elmer OPTIMA 3300DV. N_2 adsorption-desorption isotherms were obtained at 77 K on a Micromeritics Tristar 2420 analyzer. The surface areas were calculated with the Btunauer-Emmet-Teller (BET) method.

Batch treatment experiment of 4-CP

The 4-CP treatment experiment was carried out in the capped glass bottle on a shaker at room temperature.[29] First, 100 mg of 4-CP was dissolved in 1000 ml of deionized water and its pH was adjusted to 4 by adding H_2SO_4. Typically, 50 mg of as-synthesized product was added into the mixture of 4-CP solution (50 ml, pH=4) and hydrogen peroxide solution (0.5 ml, 5wt. %). From the beginning of adding the product, at the given reaction time intervals, 0.5 ml of sample was taken out from the system and 5μl *tert*-butanol was dropped into the sample at once as the reaction inhibitor. The samples were then filtered through a syringe filter (pore size=0.22 μm). For Fe@C core-shell particles, the time interval was 2 min while it was 1 min for Fe@C yolk-shell particles. For TOC measurement, one drop of 1M NaOH was added immediately to stop the reaction.

In every batch treatment experiment, the concentration of remaining 4-CP was detected by HPLC (detect limit < 0.5 mg/l). The mobile phase is a mixture of deionized water (30%) and methanol (70%). Samples were injected into the HPLC with a flow rate of 1ml/min; and the signal was detected by the UV spectrometer at the absorbance wavelength of 230 nm.

Results and discussion

We choose nonmagnetic Fe_2O_3 particles as the core and then reduce them into Fe with the carbon shell formed from polymerized RF to avoid the aggregation of Fe which is caused by its magnetic property. Our overall synthetic route is described in Scheme 1.

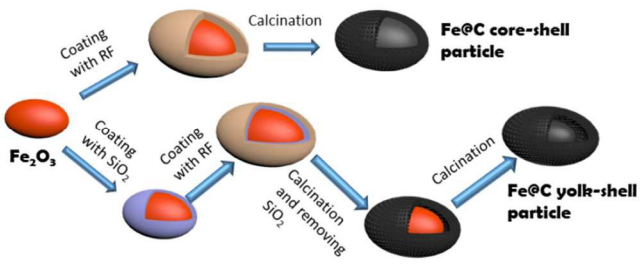

Scheme 1 Illustration of the synthesis pathway

Synthesis and characterization of Fe@C core-shell particles and Fe@C york-shell particles

In the first step, the rice-shaped Fe_2O_3 particles (Fig.1a) were synthesized by aging the solution containing $FeCl_3$ and NaH_2PO_4. Fig.1b shows a SEM image and Fig.1c shows a TEM image of the Fe_2O_3@RF core-shell particles, both of which indicate that the RF was coated around the Fe_2O_3 core uniformly. The shell grew around the core through the self-assembly of $CTMA^+Br^-$ and RF to form a uniform layer.[50] The polymer shell thickness is ca. 70 nm as reflected from Fig.1c. In the second step, the RF coated around the Fe_2O_3 core was transformed into carbon by calcination under N_2 atmosphere for 2 h at 600 °C. Since the surfactant in the RF was eliminated, microporous carbon shell were formed. In the third step, core Fe_2O_3 was reduced to Fe by the carbon shell under N_2 atmosphere at 900 °C. Finally, we got the product of Fe@C core-shell particles (Fig.1d).

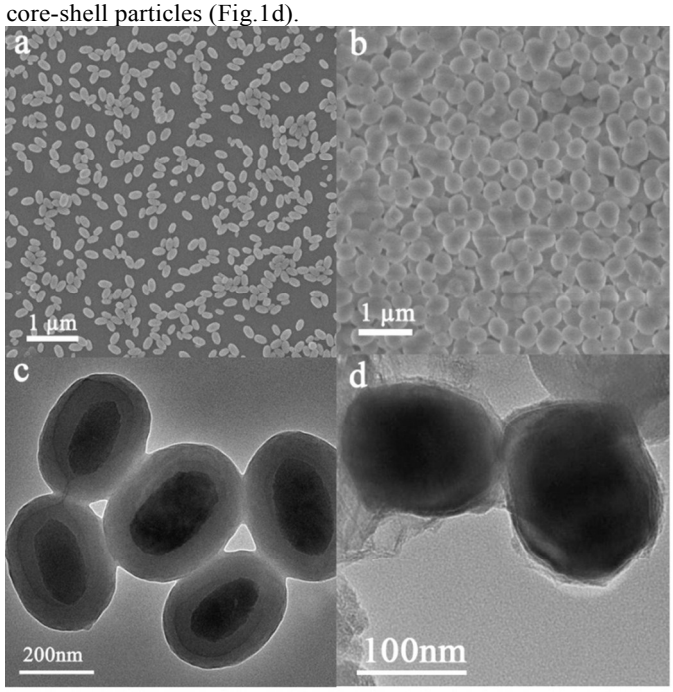

Fig.1 (a) SEM image of the rice-shaped Fe_2O_3 particles; (b) SEM image and (c) TEM image of the Fe_2O_3@RF particles; (d) TEM image of the Fe@C core-shell particles.

One of effective methods to improve the reaction activity of Fe is to increase the active sites on it. Therefore, Fe@C yolk-shell particles were designed and synthesized. In the first step of this part, the rice-shaped Fe_2O_3 particles were coated with a uniform layer of SiO_2 by the hydroxylation of TEOS (Fig.2a). The TEM image in Fig.2c indicates the thickness of the SiO_2 layer as ca. 20 nm. This SiO_2 layer is synthesized a litter thin so that the cavity won't obstruct the reduction later. And the next step is very similar with that of the former part, except using Fe_2O_3@SiO_2 as the core instead of Fe_2O_3 particles. Both Fig.2b and Fig.2c reflect that a layer of RF has been coated on the Fe_2O_3@SiO_2 uniformly and the particles are still monodisperse. As for these particles, the thickness of the RF layer is ca. 30 nm. In the third step, the RF layer is transformed into carbon

through calcination as mentioned in the former part. Then the SiO_2 layer was removed by a hydrothermal treatment using ammonia solution. In the fourth step, the core Fe_2O_3 was reduced into Fe according to the same condition as the former part. Following this, the Fe@C yolk-shell particles were obtained (Fig.2d). In the yolk-shell structure, there is a cavity between the Fe core and the C shell (Fig.S1). The HRTEM image also indicates the micropores in the carbon shell (Fig.S1).

Nitrogen adsorption-desorption isotherms are presented as Fig. S2. The BET surface area of Fe@C yolk-shell particle is 65 m^2/g, which significantly increases compared with 16 m^2/g for the Fe@C core-shell particle. So, compared with the Fe@C core-shell particles, the complete surface of the Fe core can be reached by reactants. In this way, the number of active sites in Fe@C yolk-shell particles increases much and thus the reaction activity to deal with chlorophenol is enhanced greatly.

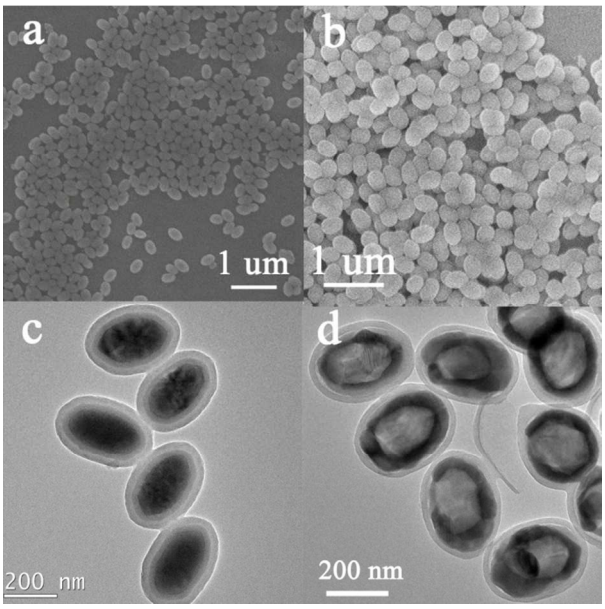

Fig.2 (a) SEM image of the Fe_2O_3@SiO_2 particles; (b) SEM image and (c) TEM image of the Fe_2O_3@SiO_2@RF particles; (d) TEM image of the Fe@C yolk-shell particles.

Fig.3a shows the XRD patterns of the Fe_2O_3 rice-shaped particles, which is obtained through forced hydrolysis of ferric chloride solution in the hydrothermal condition. The XRD peaks fit with the characteristic peaks of Fe_2O_3 very well and reveal the solid as Fe_2O_3. After calcination, as shown in Fig.3b, the patterns clearly indicate the complete reduction of Fe_2O_3 into Fe. Together with the disappearance of the diffraction peaks of Fe_2O_3, two strong and sharp peaks are observed, which can be indexed to Fe [110] and [200] respectively. For both Fe@C core-shell and Fe@C yolk-shell particles, this means the Fe_2O_3 has been reduced to Fe by their carbon shell through calcination under N_2 atmosphere. The state of the carbon shell is investigated by Raman spectrum (Fig. S3). All the peaks of G band and D band in the spectrum indicate the carbon has been graphitized in both Fe@C core-shell and Fe@C yolk-shell particle.[53-55]

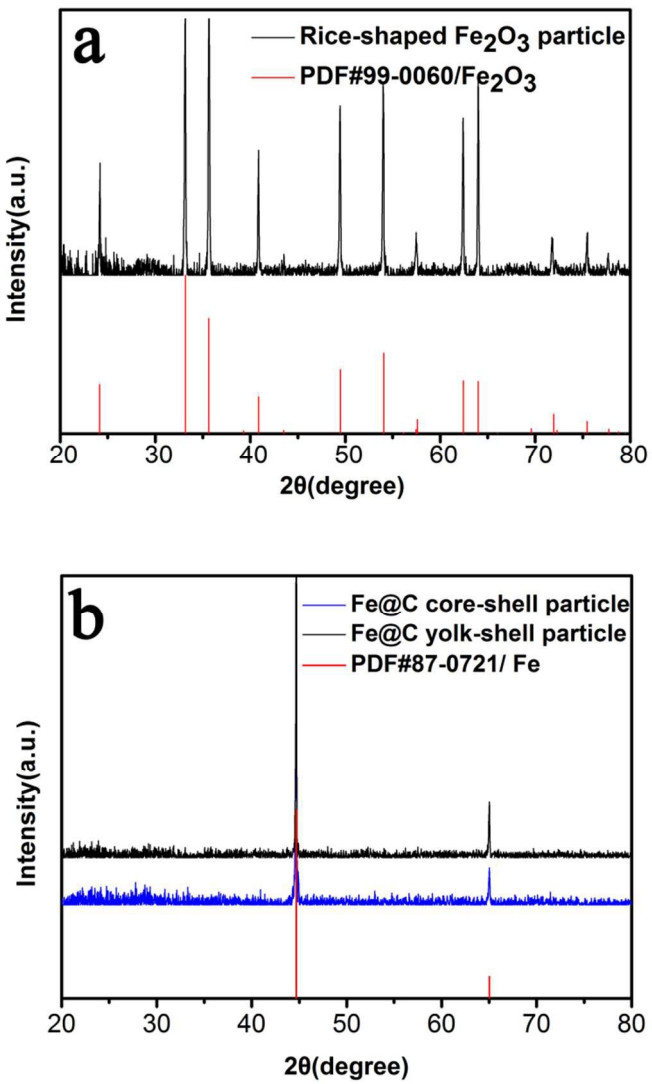

Fig. 3 XRD patterns of (a) Fe_2O_3 particles and (b) Fe@C core-shell and Fe@C yolk-shell particles

The chemical composition of these two kinds of particles were measured by the CHN elemental analysis and inductively coupled plasma mission spectroscopy. As shown in the Table 1, the proportion of Fe in Fe@C core-shell particle is 60%, while that in Fe@C yolk-shell particle is 56%. In addition, the magnetic property of the particles was tested by VSM. As shown in Fig. S4, the magnetization curves without hysteresis occurring indicates superparamagnetic behavior at room temperature for both Fe@C core-shell and Fe@C yolk-shell particle.[56, 57]

Table 1 The elemental components of Fe@C core-shell and Fe@C yolk-shell particles

Product	Carbon wt.%	Iron element wt.%
Fe@C core-shell particle	3	60
Fe@C yolk-shell particle	11	56

Chlorophenol treatment experiment

We choose the 4-CP as the target molecule to investigate the efficiency of Fe@C core-shell and Fe@C yolk-shell particles to deal with the chlorophenol. With Fe in the hydrogen peroxide solution, Fenton-like reaction can generate hydroxyl radical, which is a strong oxidant to degrade the 4-CP to aliphatic organic acid, e.g. maleic acid.[29]

PERFORMANCE AND REACTION KINETICS

We first investigate the performance of Fe@C core-shell particles to deal with 4-CP. As shown in Fig. 4a and b, it is a two-stage first-order degradation kinetic.[29, 58, 59] The first-stage is an initial slow degradation period and the following second-stage is a rapid degradation period. The k_{obs} of the first-stage is calculated to be 0.067 min^{-1} and the k_{obs} of the second-stage is 0.835 min^{-1}, where the former one is one magnitude smaller than the later one. This lower k_{obs} can be ascribed to the heterogeneous reaction, which occurs only on the iron surface and the number of generated •OH is small.[28] In the second-stage, the k_{obs} is in the similar order of magnitude to that of homogeneous Fenton system reported before.[29] So we can conclude that the rapid oxidation rate in the second-stage is mainly accredited to the homogeneous dissolved Fe^{2+}/H_2O_2 Fenton reaction, although the possible heterogeneous catalysis effect could also exist. The process of degradating 4-CP diffused from the Fe surface into the solution. In this stage, 4-CP would decrease to an absolutely low level, which is below the HPLC detection limit (< 0.5 mg/l).

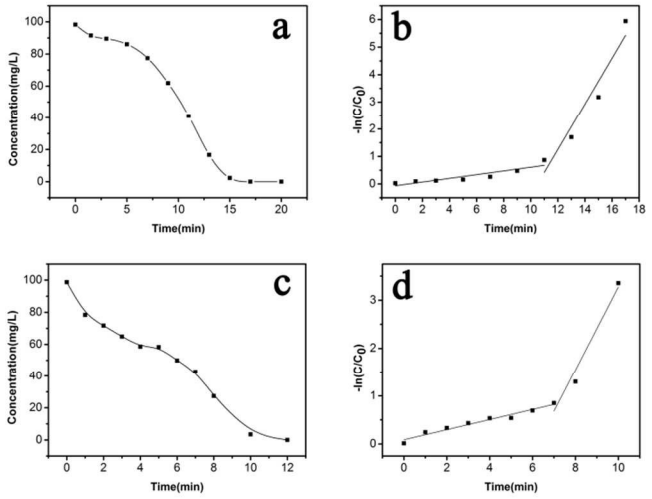

Fig.4 The degradation of 4-CP by (a and b) Fe@C core-shell particles and (c and d) Fe@C yolk-shell particles. The parameters were fixed on particles 1 mg/ml, 4-CP 100mg/L, H_2O_2 0.5‰, pH=4.

In the experiment of the degrading 4-CP catalyzed by Fe@C core-shell particle, the high performance of this particle may be attributed to its core-shell structure, which helps to avoid the serious aggregation caused by the magnetic property of Fe itself. And at the same time, the microporous carbon shell provides the pathways for 4-CP and H_2O_2 to get to the active sites on the surface of the core. So, to further improve the performance of degrading 4-CP, we design and synthesize the Fe@C yolk-shell particle.

As shown in Fig. 4c and d, the two-stage first-order degradation kinetic also applies well to the experiment of Fe@C yolk-shell particle. It also contains an initial slow first-stage and a following rapid second-stage. As shown in the Fig. 4c, the Fe@C yolk-shell particle can remove 4-CP thoroughly within 12 minutes. From the Fig. 4d, the k_{obs} of the first-stage is calculated to be 0.105 min^{-1}. Compared with that of the Fe@C core-shell particle, it increases much. The better catalytic performance of Fe@C yolk-shell particle may be attributed to its unique yolk-shell structure.[60] The cavity of the yolk-shell particle as a nanoreactor provides sufficient space and numerous available active sites for 4-CP and H_2O_2 to react on the iron core surface. So the degradation rate increases much and the reaction time of the first-stage decreases to half. Then in the second-stage, the k_{obs} is calculated to be 0.863 min^{-1}, which is similar to that of the Fe@C core-shell particle since they are both homogeneous Fenton catalytic degradation.

We compare the total organic carbon (TOC) of the 4-CP solution before and after the treatment by Fe@C yolk-shell particle. The initial TOC is 57 mg/L. After the degradation, the TOC turns to be 25 mg/L. The degree of mineralization is calculated to be about 56%, which is consistent with the reported paper.[29] The remaining TOC may ascribe to the aliphatic organic acid, e.g. maleic acid generated by oxidization of 4-CP through continuously •OH attacking.

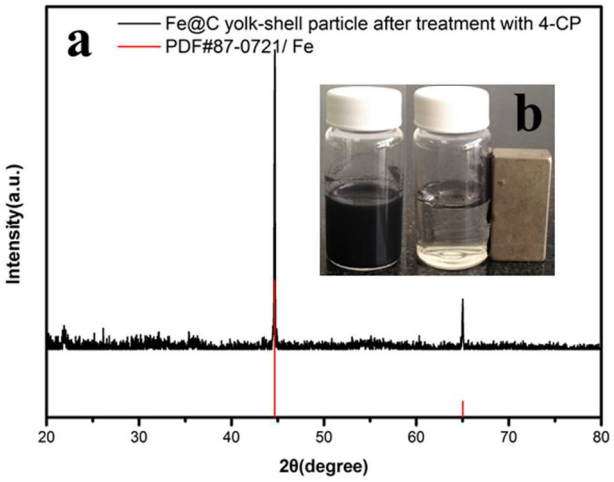

Fig.5 (a) XRD patterns of Fe@C yolk-shell particle after the treatment with 4-CP (b) Optical photograph of the reaction system before (left) and after (right) adding an external magnet.

RECYCLE AND REUSABILITY

The reusability was investigated by its repeated usage. After the batch treatment experiment, we collected the Fe@C yolk-shell particles from the reaction system easily by an external magnet (Fig. 5a) and examined the powder by XRD (Fig. 5b). The XRD patterns reveal that the particles remain zero valent iron. Therefore, we demonstrate that the oxidized Fe^{2+} or Fe^{3+} dissolves in the liquid and the solid separated from the reaction system remains zero valent iron, which makes the reusability of particles possible.

Fig.6 reveals that the particles can be successfully reused for three cycles, and the removal efficiency for every cycle is 100% complete within 15 minutes. Successive experiments have proved the reusability of the Fe@C yolk-shell particles, which makes it a promising material for potential application.

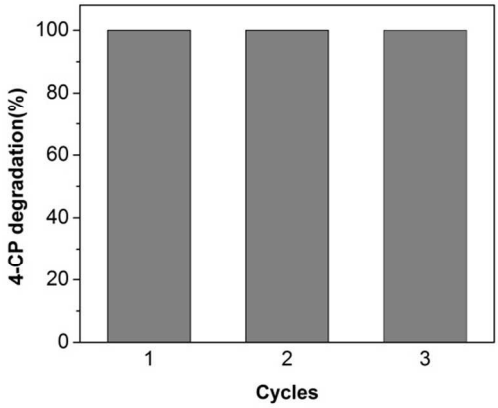

Fig.6 Degradation of 4-CP in three successive cycles with Fe@C yolk-shell particles

Regeneration

As shown in Fig.7a, after several cycles, the degradation rate of 4-CP decreases to a certain extent, which results from the oxidation of Fe on the core surface due to a long time exposure to air and water and may also ascribe to the 4-CP adsorption on the C shell. After the regeneration with calcination, Fe@C yolk-shell particles show high performance in degradation of 4-CP like the original (Fig.7a): complete removal of 4-CP within 15 min. Therefore, it can be regenerated by calcination under N_2 atmosphere since the carbon shell can reduce the core into Fe once again. We have also carried out more recycles of regeneration tests. As shown in Fig. 7b, for the former four cycles, the regenerated Fe@C yolk-shell particle performs as well as the original one: it can degrade all 4-CP in 15 min. While in the fifth cycle, the performance for degrading 4-CP becomes a little poor: the degradation rate of 4-CP in 15 min is 97.8%. This decrease of activity may be ascribed to the agglomeration after several regeneration recycles.

Conclusions

In our experiment, we have synthesized uniform Fe@C core-shell and Fe@C yolk-shell particles successfully and have shown that these particles could be a good candidate for the treatment of chlorophenol in the water. Both of these particles show promising performance on degrading 4-CP, which can remove 4-CP quickly (within 20 min) and thoroughly (the final level below the detection limit of HPLC). Especially for the Fe@C yolk-shell particles, it can remove all 4-CP within only 12 min. What's more, the magnetic property endows the particle with easy separation and good stability provides easy preservation in the air. It also has favourable reusability without any decrease of the removal efficiency. Even if its activity decreases to a certain extent after a long time exposure to air and water, it can be regenerated to its original performance again. Such studies prove the potential application of these particles in the polluted water treatment.

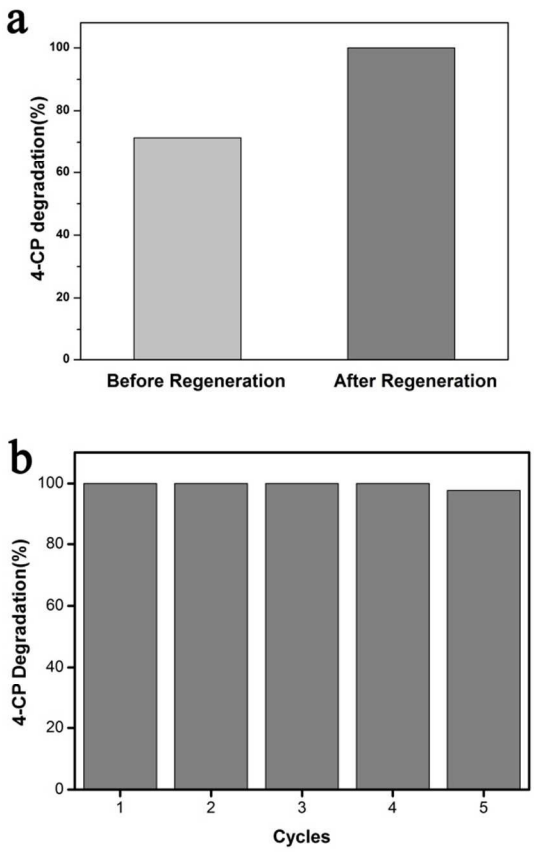

Fig.7 (a) Regeneration of Fe@C yolk-shell particle (b) Regenerations of Fe@C yolk-shell particle for successive cycles

Acknowledgements

This work was supported by the National Natural Science Foundation of China (Grant nos 21171064, 21371067 and 21373095). The authors would like to thank Dr. Yan Chen for his help on the analysis of VSM and his beneficial discussion.

Notes and references

1. I. Oller, S. Malato and J. A. Sanchez-Perez, *Sci Total Environ*, 2011, **409**, 4141-4166.
2. A. Bhatnagar and M. Sillanpaa, *Chem Eng J*, 2010, **157**, 277-296.
3. X. Gao, F. Xiao, C. Yang, J. Wang and X. Su, *J Mater Chem A*, 2013, **1**, 5831-5834.
4. M. Pera-Titus, V. García-Molina, M. A. Baños, J. Giménez and S. Esplugas, *Appl Catal B: Environ*, 2004, **47**, 219-256.
5. X. Yin, W. Liu and J. Ni, *Chem Eng J*, 2014, **248**, 89-97.

6. Z. Dong, X. Le, Y. Liu, C. Dong and J. Ma, *J Mater Chem A*, 2014, **2**, 18775-18785.
7. Z. Sun, X. Wei, Y. Han, S. Tong and X. Hu, *J Hazard Mater*, 2013, **244–245**, 287-294.
8. S. Sabhi and J. Kiwi, *Water Res*, 2001, **35**, 1994-2002.
9. D. Zhao, Y. Zheng, M. Li, S. A. Baig, D. Wu and X. Xu, *Ultrason Sonochem*, 2014, **21**, 1714-1721.
10. J. Xu, X. Lv, J. Li, Y. Li, L. Shen, H. Zhou and X. Xu, *J Hazard Mater*, 2012, **225-226**, 36-45.
11. C. K. Remucal and M. Ginder-Vogel, *Environ Sci Proc Impacts*, 2014, **16**, 1247-1266.
12. C. A. Martinez-Huitle and S. Ferro, *Chem Soc Rev*, 2006, **35**, 1324-1340.
13. X. Duan, F. Ma, Z. Yuan, L. Chang and X. Jin, *Electrochim Acta*, 2012, **76**, 333-343.
14. W. Teng, X. Li, Q. Zhao and G. Chen, *J Mater Chem A*, 2013, **1**, 9060.
15. L. C. Sim, K. H. Leong, S. Ibrahim and P. Saravanan, *J Mater Chem A*, 2014, **2**, 5315.
16. L. C. Sim, K. H. Leong, S. Ibrahim and P. Saravanan, *J Mater Chem A*, 2014, **2**, 5315-5322.
17. W. Gao, X. Sun, T. Chen, Y. Lin, Y. Chen, F. Lu and Z. Chen, *J Sep Sci*, 2012, **35**, 1967-1976.
18. A. Toth, A. Torocsik, E. Tombacz and K. Laszlo, *J Colloid Interface Sci*, 2012, **387**, 244-249.
19. M. Anbia and M. Lashgari, *Chem Eng J*, 2009, **150**, 555-560.
20. Y. Liu, Z. Zeng, G. Zeng, L. Tang, Y. Pang, Z. Li, C. Liu, X. Lei, M. Wu, P. Ren, Z. Liu, M. Chen and G. Xie, *Bioresour Technol*, 2012, **115**, 21-26.
21. M. Gomez, G. Matafonova, J. L. Gomez, V. Batoev and N. Christofi, *J Hazard Mater*, 2009, **169**, 46-51.
22. Q. Wen, T. Yang, S. Wang, Y. Chen, L. Cong and Y. Qu, *J Hazard Mater*, 2013, **244–245**, 743-749.
23. B. G. Kwon, D. S. Lee, N. Kang and J. Yoon, *Water Res*, 1999, **33**, 2110-2118.
24. M.-C. Lu, J.-N. Chen and H.-H. Huang, *Chemosphere*, 2002, **46**, 131-136.
25. M.-C. Lu, *Chemosphere*, 2000, **40**, 125-130.
26. G. Lente and J. H. Espenson, *Green Chem*, 2005, **7**, 28-34.
27. L. Wang, S.-Q. Ni, C. Guo and Y. Qian, *J Mater Chem A*, 2013, **1**, 6379.
28. F. Duan, Y. Yang, Y. Li, H. Cao, Y. Wang and Y. Zhang, *Journal of Environmental Sciences*, 2014, **26**, 1171-1179.
29. T. Zhou, Y. Li, J. Ji, F.-S. Wong and X. Lu, *Sep Purif Technol*, 2008, **62**, 551-558.
30. S. S. Wijesekara, B. F. Basnayake and M. Vithanage, *Environ Sci Pollut Res Int*, 2014, **21**, 7075-7087.
31. L. Zhou, T. L. Thanh, J. Gong, J. H. Kim, E. J. Kim and Y. S. Chang, *Chemosphere*, 2014, **104**, 155-161.
32. X. Bai, Z. F. Ye, Y. Z. Qu, Y. F. Li and Z. Y. Wang, *J Hazard Mater*, 2009, **172**, 1357-1364.
33. Z. Fang, J. Chen, X. Qiu, X. Qiu, W. Cheng and L. Zhu, *Desalination*, 2011, **268**, 60-67.
34. R. Cheng, J. L. Wang and W. X. Zhang, *J Hazard Mater*, 2007, **144**, 334-339.
35. Y. Liu, F. Yang, P. L. Yue and G. Chen, *Water Res*, 2001, **35**, 1887-1890.
36. Y. Dai, F. Li, F. Ge, F. Zhu, L. Wu and X. Yang, *J Hazard Mater*, 2006, **137**, 1424-1429.
37. Y. Li, Y. Zhang, J. Li, G. Sheng and X. Zheng, *Chemosphere*, 2013, **92**, 368-374.
38. Z. Ai, Z. Gao, L. Zhang, W. He and J. J. Yin, *Environ Sci Technol*, 2013, **47**, 5344-5352.
39. S. Xing, D. Zhao, W. Yang, Z. Ma, Y. Wu, Y. Gao, W. Chen and J. Han, *J Mater Chem A*, 2013, **1**, 1694.
40. J. Yang, W. Chen, D. Shen, Y. Wei, X. Ran, W. Teng, J. Fan, W.-x. Zhang and D. Zhao, *J Mater Chem A*, 2014, **2**, 11045.
41. S. Ikeda, S. Ishino, T. Harada, N. Okamoto, T. Sakata, H. Mori, S. Kuwabata, T. Torimoto and M. Matsumura, *Angew Chem Int Ed*, 2006, **45**, 7063-7066.
42. X. Li, A. Dhanabalan, L. Gu and C. Wang, *Adv Energy Mater*, 2012, **2**, 238-244.
43. K. Kamata, Y. Lu and Y. N. Xia, *J Am Chem Soc*, 2003, **125**, 2384-2385.
44. K. T. Lee, Y. S. Jung and S. M. Oh, *J Am Chem Soc*, 2003, **125**, 5652-5653.
45. R. Liu, S. M. Mahurin, C. Li, R. R. Unocic, J. C. Idrobo, H. Gao, S. J. Pennycook and S. Dai, *Angew Chem Int Ed*, 2011, **50**, 6799-6802.
46. A. H. Lu, T. Sun, W. C. Li, Q. Sun, F. Han, D. H. Liu and Y. Guo, *Angew Chem Int Ed Engl*, 2011, **50**, 11765-11768.
47. A. B. Fuertes, P. Valle-Vigon and M. Sevilla, *Chem Commun*, 2012, **48**, 6124-6126.
48. X. Fang, Z. Liu, M.-F. Hsieh, M. Chen, P. Liu, C. Chen and N. Zheng, *Acs Nano*, 2012, **6**, 4434-4444.
49. M. Ozaki, S. Kratohvil and E. Matijević, *J Colloid Interface Sci*, 1984, **102**, 146-151.
50. B. Guan, X. Wang, Y. Xiao, Y. Liu and Q. Huo, *Nanoscale*, 2013, **5**, 2469-2475.
51. Y. Wang, B. Li, C. Zhang, X. Song, H. Tao, S. Kang and X. Li, *Carbon*, 2013, **51**, 397-403.
52. W. Chen, X. L. Pan, M. G. Willinger, D. S. Su and X. H. Bao, *J Am Chem Soc*, 2006, **128**, 3136-3137.
53. Y. Cheng, C. Xu, L. Jia, J. D. Gale, L. Zhang, C. Liu, P. K. Shen and S. P. Jiang, *Appl Catal B: Environ*, 2015, **163**, 96-104.
54. M. S. Dresselhaus, G. Dresselhaus, R. Saito and A. Jorio, *Physics Reports*, 2005, **409**, 47-99.
55. U. J. Kim, C. A. Furtado, X. M. Liu, G. G. Chen and P. C. Eklund, *J Am Chem Soc*, 2005, **127**, 15437-15445.
56. M. A. S. Boff, R. Hinrichs, B. Canto, F. Mesquita, D. L. Baptista, G. L. F. Fraga and L. G. Pereira, *Appl Phys Lett*, 2014, **105**, 143112.
57. R.-J. Chung, *J Med Biol Eng*, 2014, **34**, 251.
58. Y. Du, M. Zhou and L. Lei, *J Hazard Mater*, 2006, **136**, 859-865.

59. L. Xu and J. Wang, *Appl Catal B: Environ*, 2012, **123-124**, 117-126.
60. T. Zeng, X. Zhang, S. Wang, Y. Ma, H. Niu and Y. Cai, *Chem Eur J*, 2014, **20**, 6474-6481.

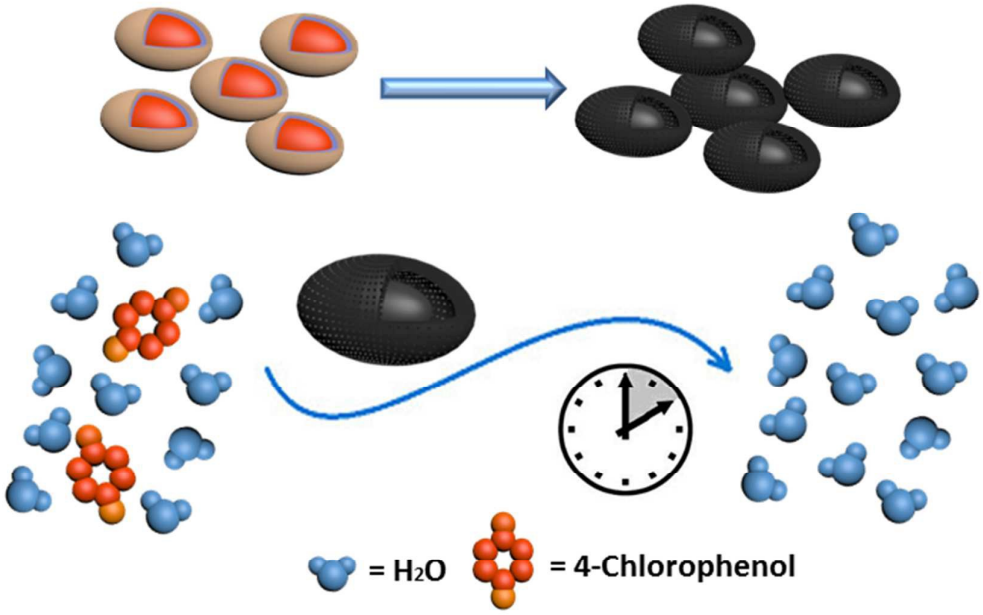

Fe@C yolk-shell particles were synthesized by reducing the core with its own carbon shell to achieve the effective removal towards 4-chlorophenol from the water.